Online ISSN 1848-3380, Print ISSN 0005-1144
ATKAFF 57(3), 749–760(2016)

Nicolás González, Oscar Salas-Peña, Jesus de León-Morales, Sergio Rosales, Vicente Parra-Vega

Observer-based Integral Sliding Mode Approach for Bilateral Teleoperation with Unknown Time Delay

DOI 10.7305/automatika.2017.02.1399
UDK [681.532.075:517.977.15]:621.865.8-519-022.215

Original scientific paper

This paper deals with force-reflecting control design for teleoperation of bilateral robots under unknown constant time delay. The proposed impedance teleoperator control is based on integral sliding mode approaches, avoiding undesirable chattering effect. With the aim of implementing the proposed controller and taking into account that only position measurement is available, a Nonlinear Observer based on Super Twisting Algorithm is proposed to estimate velocity and acceleration in the slave side of the teleoperation system. Furthermore, owing to the finite-time convergence properties of the observer, the proposed control scheme guarantees robust tracking under unknown constant time delay. Experimental results illustrate the effectiveness of the proposed scheme.

Key words: Teleoperation, Sliding Mode Control, Observers

Integralno upravljanje u kliznom režimu zasnovano na observeru za bilateralnu teleoperaciju s nepoznatim kašnjenjem. Ovaj rad bavi se upravljanjem zasnovanim na reflektiranju sile za teleoperaciju bilateralnih robota s nepoznatnim konstantnim kašnjenjem. Predloženo upravljanje impedancijom zasnovano je na cjelovitom pristupu kliznom režimu uz izbjegavanje efekta "chatteringa". S ciljem implementacije predloženog upravljanja i uzimajući u obzir da je dostupno samo mjerenje pozicije, za estimaciju brzine i akceleracije na "slave" strani teleoperacijskog sustava koristi se nelinearni observer zasnovan na "Super Twisting" algoritmu. Nadalje, zbog konačnog vremena konvergencije observera, predloženo upravljanje garantira robusno praćenje uz nepoznato konstantno kašnjenje. Eksperimentalni rezultati ilustriraju učinkovitost predloženog rješenja.

Ključne riječi: teleoperacija, upravljanje u kliznom režimu, observeri

Teleoperation system stability is mainly affected by communication time delays [1], even if the dynamics of the system are known and the states are available. In bilateral teleoperation, five interconnected elements are distinguished: the *human operator* driving the *master robot* in order to generate the position, velocity and force commands; these commands are sent as desired references through the *communication channel* to the *slave robot*, as shown in Figure 1. On the other hand, when the slave robot interacts with the *environment*, it reflects the contact force through the master robot to the human operator, which reacts to generate next command. The fidelity of such force displayed defines how human user perceives the interaction.

The main purpose in teleoperation is to achieve *transparency*, which is measured in terms of trajectory tracking during free, holding stability under any operating conditions and for any possible environment. Transparency has been considered as a requirement for critical applications (see [2, 3]). Furthermore, transparency is better assessed in terms of the matching degree between the impedance perceived by the operator and the environment impedance.

Several schemes have been proposed to deal with the bilateral teleoperation problem under time delay introduced by communication channels. In [4, 5], a scattering-based approach PD-like, under the assumption that human operator force and the contact environment are defined passives, position tracking is ensured. An adaptive scheme based on passivity is considered in [6], where unknown parameters are estimated to guarantee position tracking. On the other hand, a different approach considers the impedance control in teleoperated systems [7]. Sliding mode control techniques represent an interesting approach, where robust tracking is achieved even under parametric uncertainties (see [9,10]). In [11], sliding modes have been proposed for teleoperation, including desired impedance scheme with a linear observer. Velocity measurement improves performance in teleoperation as the velocity of master is considered as a reference for slave system. Moreover, this characteristic aware the user in case of the slave devi-

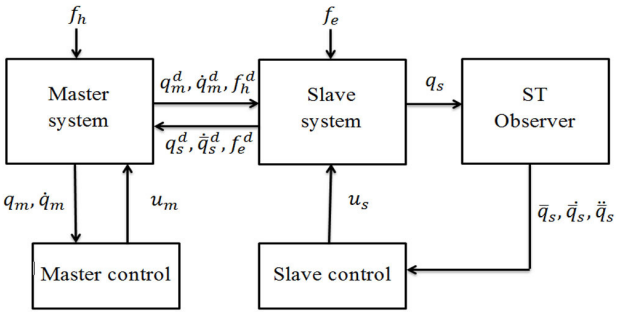

Fig. 1: A block diagram of bilateral teleoperation

ates from target.

Impedance control requires velocity and acceleration measurements in order to implement a desired impedance [8]. However, in order to avoid expensive and bulky sensors which may add noise to the system, the use of observers represents an interesting solution. For example, observer-based controls for a class of triangular nonlinear systems are presented in [16, 17], wherein stabilization is guaranteed despite the size of delay. Nonetheless, convergence of the estimation errors of these observers is asymptotical. Super Twisting Observers represent an attractive methodology [18,20,21], due to its robustness and furthermore its finite-time convergence property, the separation principle is accomplished and thus controller and observer can be designed separately.

Contribution. In this paper, an integral second order sliding mode impedance control for the slave system is designed to track position, velocity and contact force trajectories of master system, subject to unknown constant time delay in communication system. Moreover, in order to implement the proposed controller, velocity and acceleration are provided by means of a Super Twisting Observer, which is robust in presence of unknown constant time delays. Furthermore, the closed-loop system guarantees time delay transparency. Experimental results illustrate the feasibility and performance of the proposed scheme in presence of measurement noise, for different constant time delays.

Paper structure. This paper is organized as follows: In Section 2, the dynamical model of a bilateral teleoperated system is introduced. Section 3 addresses the design of a second order sliding mode impedance control for the slave system to track the master trajectories. Moreover, a Super Twisting Observer for estimating velocity and acceleration of the slave system is designed in order to implement the proposed controller, in Section 4. Experimental results for validating the proposed control scheme are given in Section 5. Finally, conclusions of this work are drawn.

1 DYNAMIC TELEOPERATION MODEL AND THE CONTROL PROBLEM

Now, the mathematical models describing the dynamical behavior of master and slave system are introduced. With this aim, consider the dynamics of a master/slave system modeled with the Euler-Lagrange formalism are given by

$$\mathbf{M}_m(\mathbf{q}_m)\ddot{\mathbf{q}}_m + \mathbf{C}_m(\mathbf{q}_m, \dot{\mathbf{q}}_m)\dot{\mathbf{q}}_m + \mathbf{g}_m(\mathbf{q}_m) = \tau_h + \mathbf{u}_m, \quad (1)$$

$$\mathbf{M}_s(\mathbf{q}_s)\ddot{\mathbf{q}}_s + \mathbf{C}_s(\mathbf{q}_s, \dot{\mathbf{q}}_s)\dot{\mathbf{q}}_s + \mathbf{g}_s(\mathbf{q}_s) = \mathbf{u}_s - \tau_e, \quad (2)$$

where $\mathbf{q}_i$, $\dot{\mathbf{q}}_i$, $\ddot{\mathbf{q}}_i \in \mathbb{R}^n$ are the joint generalized positions, velocities and acceleration vectors, respectively; $\mathbf{M}_i(\mathbf{q}_i) \in \mathbb{R}^{n\times n}$ stands for the inertia matrices; $\mathbf{C}_i(\mathbf{q}_i, \dot{\mathbf{q}}_i) \in \mathbb{R}^{n\times n}$ represent the Coriolis and centrifugal effects, arising from the Christoffel symbols of the first kind; $\mathbf{g}_i(\mathbf{q}_i) \in \mathbb{R}^n$ denotes the gravity force; and $\mathbf{u}_i \in \mathbb{R}^n$ stands for the control signals. Subscript i stands for either m or s denoting the master or slave, respectively. Torques $\tau_h = J(\mathbf{q}_m)^T\mathbf{f}_h$ and $\tau_e = J(\mathbf{q}_s)^T\mathbf{f}_e$, are smooth bounded torque inputs of the human operator on the master side and the environmental contact in the slave side, respectively. These torques arise as consequence of the human force $\mathbf{f}_h$ applied at master side and environmental force $\mathbf{f}_e$ applied at slave side, where $J(\cdot)$ is assumed a well-posed Jacobian.

Signals for each system are sent through the communication channel having a time delay, represented here by the superscript-d, are given as follows, $\mathbf{q}_s^d(t) := \mathbf{q}_m(t - T_1)$, $\dot{\mathbf{q}}_s^d(t) := \dot{\mathbf{q}}_m(t-T_1)$, $\ddot{\mathbf{q}}_s^d(t) := \ddot{\mathbf{q}}_m(t-T_1)$, $\mathbf{f}_h^d(t) := \mathbf{f}_h(t - T_1)$ and $\mathbf{f}_e^d(t) := \mathbf{f}_e(t - T_2)$, where $T_1 > 0$ and $T_2 > 0$ stand for bounded constant and unknown time delays induced by the communication channel. These signals are scaled by constant factors or transformed to handle kinematic and workspace dissimilarities. In this paper, we assume without loss of generality that scaling factors $\mathbf{K}_p, \mathbf{K}_f$ are diagonal positive definite constant matrices for position and force variables, respectively, and $T_1 = T_2$.

Notice that, the time delay is assumed to be unknown and constant. Furthermore, position is available by measurement. Then the control objective can be established.

Control Objective. To design an impedance control law u_i, $i = m, s$; such that the trajectories converge to desired impedance manifold for the master and slave robot systems. Furthermore, the desired position in the slave robot is reached when no environmental force is presented.

2 IMPEDANCE CONTROL DESIGN

In this section, an impedance controller and a sliding mode based impedance controller are designed for master

and slave systems, respectively. These controllers are designed based on position-force teleoperation.

The master robot operator typically involves a haptic interface designed to display force and read precisely the commanded position with high-end robots, whose dynamical models and their nominal parameters are assumed to be known. However, this is not the case for slave robots, where an experimental or industrial robot is in place. In order to establish a dynamic relationship between position and force, impedance sliding surfaces for master and slave robots are defined. With this aim, a torque controller for master system and a passivity-based sliding mode control for slave are designed.

2.1 Impedance control for master system

In order to expand the number of applications of robots, besides controlling the motion, it is also necessary to control the forces of interaction between the manipulator and the environment. A distinction between impedance control and conventional approaches to bilateral teleoperation systems is that the impedance control attempts to implement a dynamical relation between robot variables such as end-point position and force rather than just control these variables.

Now, consider the following controller

$$\begin{aligned}\mathbf{u}_m &= \mathbf{C}_m(\mathbf{q}_m,\dot{\mathbf{q}}_m)\dot{\mathbf{q}}_m + \mathbf{g}(\mathbf{q}_m) - J^T(\mathbf{q}_m)\mathbf{f}_h \\ &\quad +\mathbf{M}_m^*\{J^T(\mathbf{q}_m)\Delta\mathbf{f}_h - \bar{\mathbf{C}}_m\dot{\mathbf{q}}_m - \bar{\mathbf{K}}_m\mathbf{q}_m\},\end{aligned} \tag{3}$$

where $\Delta\mathbf{f}_h = \mathbf{f}_h - \mathbf{f}_{hd}$ stands for the force tracking error on master system, and $\mathbf{f}_{hd} = \mathbf{K}_f\mathbf{f}_e^d$ are the scaled desired force for the user, $\mathbf{M}_m^* = \mathbf{M}_m(\mathbf{q}_m)\bar{\mathbf{M}}_m^{-1}$, and $\bar{\mathbf{M}}_m$, $\bar{\mathbf{C}}_m$, $\bar{\mathbf{K}}_m > 0$ are the desired inertia, damping, and stiffness, respectively, of a desired impedance. We now have the following result.

Proposition 2.1. Consider the master system (1) in closed-loop with the control (3). Then, closed-loop trajectories are all bounded, with exponential convergence of the impedance master invariant manifold

$$I_h = \bar{\mathbf{M}}_m(\mathbf{q}_m)\ddot{\mathbf{q}}_m + \bar{\mathbf{C}}_m\dot{\mathbf{q}}_m + \bar{\mathbf{K}}_m\mathbf{q}_m - J^T(\mathbf{q}_m)\Delta\mathbf{f}_h \equiv 0, \tag{4}$$

where feedback gains are properly chosen.

Proof. Substituting (3) into (1) we obtain the impedance master invariant manifold (4), which can be rewritten as follows

$$\bar{\mathbf{M}}(\mathbf{q}_m)\ddot{\mathbf{q}}_m + \bar{\mathbf{C}}_m\dot{\mathbf{q}}_m + \bar{\mathbf{K}}_m\mathbf{q}_m = J^T(\mathbf{q}_m)\Delta\mathbf{f}_h, \tag{5}$$

having a linear time-invariant second order homogeneous differential equation with forced input $\Delta\mathbf{f}_h$. In free motion case, $\Delta\mathbf{f}_h = 0$ then (5) attains a unique global equilibrium at $(\mathbf{q}_m, \dot{\mathbf{q}}_m) = (0, 0)$. On the other hand, in case of contact, a torque proportional to a force $\mathbf{f}_{hd}$ is displayed on the master system (i.e. at the hand of the human user). Notice that (5) attains to a Bounded Input-Bounded Output (BIBO) stability for bounded input $\Delta\mathbf{f}_h \in \mathcal{L}_\infty$. Moreover, (5) is obtained without measuring the time delay $T_1 > 0$, although under the assumption of $\dot{T}_1 = 0$. **QED**

Remark 1. Controller (3) imposes a desired impedance dynamics in the master teleoperator by canceling the physical dynamic from the master system and replacing it by a desired one, whose parameters are selected according to the physical properties of the teleoperator master robot. Furthermore, when $\bar{\mathbf{M}}_m = \bar{\mathbf{M}}_m(\mathbf{q}_m) = \mathbf{M}_m(\mathbf{q}_m)$, then $\mathbf{f}_h$ is no longer needed, implying that impedance is dominated by the real inertial matrix of the slave, which may be convenient in some tasks to increase the awareness of the user.

2.2 Sliding mode based impedance controller for the slave robot

2.2.1 Nominal parameters case

Using a similar rationale to design the master controller, an integral second order sliding mode approach is considered for the slave robot in order to drive a desired impedance behavior modulated by the environmental contact forces on the slave side. Furthermore, the proposed controller must be robust in presence of unknown time delay [11]. To this end, consider the desired slave impedance

$$\bar{\mathbf{M}}_s\ddot{\tilde{\mathbf{q}}}_s + \bar{\mathbf{C}}_s\dot{\tilde{\mathbf{q}}}_s + \bar{\mathbf{K}}_s\tilde{\mathbf{q}}_s = -J^T(\mathbf{q}_s)\mathbf{f}_e, \tag{6}$$

where $\bar{\mathbf{M}}_s$, $\bar{\mathbf{C}}_s$, $\bar{\mathbf{K}}_s > 0$ are the desired inertia, damping, and stiffness for the slave robot, respectively; and $\tilde{\mathbf{q}}_s := \mathbf{q}_s - \mathbf{K}_p\mathbf{q}_m^d$, $\dot{\tilde{\mathbf{q}}}_s := \dot{\mathbf{q}}_s - \mathbf{K}_p\dot{\mathbf{q}}_m^d$, $\ddot{\tilde{\mathbf{q}}}_s := \ddot{\mathbf{q}}_s - \mathbf{K}_p\ddot{\mathbf{q}}_m^d$, are the slave tracking errors for position, velocity and acceleration, respectively. Thus, the controller must be able to drive a closed-loop equilibrium at $I_e = 0$, from (6),

$$\mathbf{I}_e = \bar{\mathbf{M}}_s\ddot{\tilde{\mathbf{q}}}_s + \bar{\mathbf{C}}_s\dot{\tilde{\mathbf{q}}}_s + \bar{\mathbf{K}}_s\tilde{\mathbf{q}}_s + J^T(\mathbf{q}_s)\mathbf{f}_e. \tag{7}$$

Now, with the purpose of reaching the invariant manifold (7) in closed loop, consider the following controller

$$\begin{aligned}\mathbf{u}_s &= \mathbf{M}_s(\mathbf{q}_s)\mathbf{K}_p\bar{\mathbf{M}}_m^{-1}\Psi - \mathbf{M}_s(\mathbf{q}_s)\bar{\mathbf{M}}_s^{-1}\Upsilon + \mathbf{g}_s(\mathbf{q}_s) \\ &\quad +\mathbf{C}_s(\mathbf{q}_s,\dot{\mathbf{q}}_s)\dot{\mathbf{q}}_s + J^T(\mathbf{q}_s)\mathbf{f}_e - \mathbf{K}_g\Omega,\end{aligned} \tag{8}$$

where

$$\Psi = -\bar{\mathbf{C}}_m\dot{\mathbf{q}}_m^d - \bar{\mathbf{K}}_m\mathbf{q}_m^d - J^T(\mathbf{q}_m)\mathbf{K}_f\mathbf{f}_e^{dd}, \tag{9}$$

$$\Upsilon = \bar{\mathbf{C}}_s\dot{\tilde{\mathbf{q}}}_s + \bar{\mathbf{K}}_s\tilde{\mathbf{q}}_s + J^T(\mathbf{q}_s)\mathbf{f}_e + \mathbf{K}_i\int_0^t sign(\mathbf{I}_e(\tau))d\tau, \tag{10}$$

$$\Omega = \int_0^t \mathbf{I}_e(\tau)d\tau + \mathbf{K}_i \int_0^t \int_0^\sigma sign(\mathbf{I}_e(\tau))d\tau d\sigma, \quad (11)$$

for $\mathbf{K}_i > 0$ a diagonal matrix, $\mathbf{f}_e^{dd} = \mathbf{f}_e(t - 2T_1)$ the measurement of the environmental force after two readings, whatever the unknown time delay T_1 is; $\mathbf{K}_g > 0$, and $sign(\cdot)$ is the discontinuous signum function.

Proposition 2.2. Consider the slave system (2) in closed-loop with the control (8). Then, closed-loop trajectories are all bounded, with exponential convergence toward $\Omega = 0$, thus an integral second order sliding mode at $\mathbf{I}_e = 0$, consequently there arises in finite-time the desired impedance (7) as the unique global invariant equilibrium manifold. Hence, under proper tuning of desired impedance gains $\bar{\mathbf{M}}_s, \bar{\mathbf{C}}_s, \bar{\mathbf{K}}_s$, impedance tracking is assured.

Proof. Consider system (2) in closed-loop with (8), then it follows that

$$\begin{aligned}\mathbf{M}_s(\mathbf{q}_s)\ddot{\mathbf{q}}_s = -\mathbf{M}_s(\mathbf{q}_s)\mathbf{K}_p\bar{\mathbf{M}}_m^{-1}\Big\{\bar{\mathbf{C}}_m\dot{\mathbf{q}}_m^d + J^T(\mathbf{q}_m)\mathbf{K}_f\mathbf{f}_e^{dd} \\ +\bar{\mathbf{K}}_m\mathbf{q}_m^d\Big\} - \mathbf{M}_s(\mathbf{q}_s)\bar{\mathbf{M}}_s^{-1}\Big\{\bar{\mathbf{C}}_s\dot{\tilde{\mathbf{q}}}_s + \bar{\mathbf{K}}_s\tilde{\mathbf{q}}_s \\ +\mathbf{K}_i\int_0^t sign(\mathbf{I}_e(\tau))d\tau + J^T(\mathbf{q}_s)\mathbf{f}_e\Big\} - \mathbf{K}_g\Omega. \quad (12)\end{aligned}$$

By considering the equation (4) delayed, it follows that

$$\bar{\mathbf{M}}_m\ddot{\mathbf{q}}_m^d \equiv -\bar{\mathbf{C}}_m\dot{\mathbf{q}}_m^d - \bar{\mathbf{K}}_m\mathbf{q}_m^d + J^T(\mathbf{q}_m)\Delta\mathbf{f}_h^d,$$

where $\Delta\mathbf{f}_h^d = -\mathbf{K}_f\mathbf{f}_e^{dd}$. Taking into account the slave tracking errors for position, velocity and acceleration: $\tilde{\mathbf{q}}_s := \mathbf{q}_s - \mathbf{K}_p\mathbf{q}_m^d$, $\dot{\tilde{\mathbf{q}}}_s := \dot{\mathbf{q}}_s - \mathbf{K}_p\dot{\mathbf{q}}_m^d$, $\ddot{\tilde{\mathbf{q}}}_s := \ddot{\mathbf{q}}_s - \mathbf{K}_p\ddot{\mathbf{q}}_m^d$; and furthermore multiplying by $\bar{\mathbf{M}}_s\mathbf{M}_s^{-1}$ equation (12) can be rewritten as

$$\begin{aligned}\bar{\mathbf{M}}_s\ddot{\tilde{\mathbf{q}}}_s + \bar{\mathbf{C}}_s\dot{\tilde{\mathbf{q}}}_s + \bar{\mathbf{K}}_s\tilde{\mathbf{q}}_s + J^T(\mathbf{q}_s)\mathbf{f}_e \\ +\mathbf{K}_i\int_0^t sign(\mathbf{I}_e(\tau))d\tau + \bar{\mathbf{M}}_s\mathbf{M}_s^{-1}\mathbf{K}_g\Omega \equiv 0. \quad (13)\end{aligned}$$

Moreover, from (7), equation (13) is expressed as

$$\mathbf{I}_e + \mathbf{K}_i\int_0^t sign(\mathbf{I}_e(\tau))d\tau = -\bar{\mathbf{M}}_s\mathbf{M}_s^{-1}\mathbf{K}_g\Omega. \quad (14)$$

Furthermore, by taking the time derivative of (11), from equation (14) it follows that

$$\dot{\Omega} = -\bar{\mathbf{M}}_s\mathbf{M}_s^{-1}\mathbf{K}_g\Omega. \quad (15)$$

Now, let us define the following Lyapunov function

$$V_1(\Omega) = \tfrac{1}{2}\Omega^T\Omega. \quad (16)$$

Then, its time derivative is given by

$$\begin{aligned}\dot{V}_1(\Omega) &= -\Omega^T\dot{\Omega}, \\ &= -\Omega^T\bar{\mathbf{M}}_s\mathbf{M}_s^{-1}\mathbf{K}_g\Omega, \\ &\leq -\mu V_1(\Omega), \quad (17)\end{aligned}$$

where $\mu = 2\lambda_{min}\{\mathbf{M}_s\mathbf{K}_g\}$. It follows that

$$\begin{aligned}\tfrac{1}{2}\left\|\Omega(t)\right\|^2 &= V_1(\Omega(t)) \leq V_1(\Omega(t_0))e^{-2\mu(t-t_0)}, \\ &= \tfrac{1}{2}\left\|\Omega(t_0)\right\|^2 e^{-2\mu(t-t_0)},\end{aligned}$$

which exhibits exponential convergence to $\Omega = 0$, with exponentially vanishing functions $(\dot{\Omega}, \ddot{\Omega}) = (0, 0)$.

Defining the following Lyapunov function $V_1(\mathbf{I}_e) = \frac{1}{2}\mathbf{I}_e^T\mathbf{I}_e$, and taking the time derivative, it follows that

$$\dot{V}_1(\mathbf{I}_e) = \mathbf{I}_e^T\dot{\mathbf{I}}_e < -\nu \parallel \mathbf{I}_e \parallel, \quad (18)$$

where

$$\dot{\mathbf{I}}_e = -\mathbf{K}_i sign(\mathbf{I}_e) + \ddot{\Omega}, \quad (19)$$

is obtained from (14)-(15). $\nu = \lambda_{min}(\mathbf{K}_i) - c_0$, for c_0 the upper bound of $\ddot{\Omega}$. Thus, if $\lambda_{min}(\mathbf{K}_i) > c_0$, then $\nu > 0$. Next, equation (18) can be rewritten as

$$\begin{aligned}\dot{V}_1(\mathbf{I}_e) &\leq -\nu \parallel \mathbf{I}_e \parallel, \quad (20) \\ \dot{V}_1(\mathbf{I}_e) &\leq -\nu\sqrt{V(\mathbf{I}_e)}. \quad (21)\end{aligned}$$

Integrating (21), we have

$$\sqrt{V_1(t, \mathbf{I}_e)} \leq \sqrt{V_1(t_0, \mathbf{I}_e)} - \frac{\nu}{2}t. \quad (22)$$

Let $\sqrt{V_1(t_0, \mathbf{I}_e)} - \frac{\nu}{2}t_F = 0$, then the convergence time t_F is given by

$$t_F = \frac{2\sqrt{V_1(t_0, \mathbf{I}_e)}}{\nu}. \quad (23)$$

Therefore, for $t > t_F$ we have $V_1(\mathbf{I}_e(t)) = 0$. **QED**

2.2.2 Uncertain parameters case

In real-world systems, parameters of the plant are not exactly known, even if measured, they can deviate from their nominal values. With the aim of overcoming parametric uncertainties a robust controller that ensures stability properties of Proposition 2.2 is derived. Thus, consider the following controller for the slave robot

$$\begin{aligned}\mathbf{u}_s = \hat{\mathbf{M}}_s(\mathbf{q}_s)\mathbf{K}_p\bar{\mathbf{M}}_m^{-1}\Psi - \hat{\mathbf{M}}_s(\mathbf{q}_s)\bar{\mathbf{M}}_s^{-1}(\mathbf{q}_s)\Upsilon \\ +\hat{\mathbf{C}}_s\dot{\mathbf{q}}_s + \mathbf{g}_s(\mathbf{q}_s) + J^T(\mathbf{q}_s)\mathbf{f}_e - \mathbf{K}_g\Omega, \quad (24)\end{aligned}$$

where $\hat{(\cdot)}$ denotes nominal value of $(\cdot)$. Then, following proposition can be established.

Proposition 2.3. Consider the slave system (2) in closed-loop with the control (24). Thus, closed-loop trajectories are all bounded, with boundedness of Ω and its derivatives, such that an integral second order sliding mode arises at $\mathbf{I}_e = 0$, achieving in finite-time the desired

impedance (7) as the unique global invariant equilibrium manifold.

Proof. Consider system (2) in closed-loop with the controller (24), then it follows that

$$\begin{aligned}&\mathbf{M}_s(\mathbf{q}_s)\ddot{\mathbf{q}}_s + \mathbf{C}_s(\mathbf{q}_s,\dot{\mathbf{q}}_s)\dot{\mathbf{q}}_s + \mathbf{g}_s(\mathbf{q}_s) = \\ &\hat{\mathbf{M}}_s\mathbf{K}_p\ddot{\mathbf{q}}_m^d - \mathbf{K}_g\Omega + \hat{\mathbf{C}}_s\dot{\mathbf{q}}_s - \hat{\mathbf{M}}_s\bar{\mathbf{M}}_s^{-1}\Big\{\bar{\mathbf{C}}_s\dot{\tilde{\mathbf{q}}}_s + \bar{\mathbf{K}}_s\tilde{\mathbf{q}}_s \\ &+J^T(\mathbf{q}_s)\mathbf{f}_e + \mathbf{K}_i\textstyle\int_0^t sign(\mathbf{I}_e(\tau))d\tau\Big\} + \hat{\mathbf{g}}_s\end{aligned} \tag{25}$$

thus, by adding and subtracting the term $\bar{\mathbf{M}}_s\ddot{\tilde{\mathbf{q}}}_s$ and rearranging terms, it follows that

$$\begin{aligned}&\mathbf{M}_s\ddot{\mathbf{q}}_s + (\mathbf{C}_s - \hat{\mathbf{C}}_s)\dot{\mathbf{q}}_s + (\mathbf{g}_s - \hat{\mathbf{g}}_s) = \\ &-\hat{\mathbf{M}}_s\bar{\mathbf{M}}_s^{-1}\Big\{\mathbf{I}_e + \mathbf{K}_i\textstyle\int_0^t sign(\mathbf{I}_e(\tau))d\tau\Big\} - \hat{\mathbf{M}}_s(\mathbf{q}_s)\mathbf{K}_p\ddot{\mathbf{q}}_m^d \\ &-\hat{\mathbf{M}}_s(\ddot{\mathbf{q}}_s - \mathbf{K}_p\ddot{\mathbf{q}}_m^d) - \mathbf{K}_g\Omega,\end{aligned} \tag{26}$$

After simplification

$$\begin{aligned}&(\mathbf{M}_s - \hat{\mathbf{M}}_s)\ddot{\mathbf{q}}_s + (\mathbf{C}_s - \hat{\mathbf{C}}_s)\dot{\mathbf{q}}_s + (\mathbf{g}_s - \hat{\mathbf{g}}_s) = \\ &-\hat{\mathbf{M}}_s\bar{\mathbf{M}}_s^{-1}\Big\{\mathbf{I}_e + \mathbf{K}_i\textstyle\int_0^t sign(\mathbf{I}_e(\tau))d\tau\Big\} - \mathbf{K}_g\Omega,\end{aligned} \tag{27}$$

The mismatch due to the parametric uncertainty can be modeled by the linearly parameterizable form

$$(\mathbf{M}_s-\hat{\mathbf{M}}_s)\ddot{\mathbf{q}}_s+(\mathbf{C}_s-\hat{\mathbf{C}}_s)\dot{\mathbf{q}}_s+(\mathbf{g}_s-\hat{\mathbf{g}}_s) = \bar{Y}(\ddot{\mathbf{q}}_s,\dot{\mathbf{q}}_s,\mathbf{q}_s)\tilde{\Theta}, \tag{28}$$

where $\bar{Y}(\ddot{\mathbf{q}}_s,\dot{\mathbf{q}}_s,\mathbf{q}_s)$ denote the regressor and $\tilde{\Theta}$ is the error vector between the inertia parameters Θ (such as link masses, moments of inertia, etc.) and their estimated values $\hat{\Theta}$. Thus, equation (27) can be expressed as

$$\bar{Y}\tilde{\Theta} = -\hat{\mathbf{M}}_s\bar{\mathbf{M}}_s^{-1}\left\{\mathbf{I}_e + \mathbf{K}_i\int_0^t sign(\mathbf{I}_e(\tau))d\tau\right\} - \mathbf{K}_g\Omega, \tag{29}$$

By adding and subtracting term $\bar{\mathbf{M}}_s\mathbf{M}_s^{-1}\mathbf{K}_g\Omega$ into equation (29), it follows that

$$\begin{aligned}\bar{Y}\tilde{\Theta} &= -\hat{\mathbf{M}}_s\bar{\mathbf{M}}_s^{-1}\Big\{\mathbf{I}_e + \mathbf{K}_i\textstyle\int_0^t sign(\mathbf{I}_e(\tau))d\tau \\ &\quad +\bar{\mathbf{M}}_s\mathbf{M}_s^{-1}\mathbf{K}_g\Omega - \bar{\mathbf{M}}_s\mathbf{M}_s^{-1}\mathbf{K}_g\Omega\Big\} - \mathbf{K}_g\Omega,\end{aligned} \tag{30}$$

From equation (14), it is clear that $\mathbf{I}_e + \mathbf{K}_i\int_0^t sign(\mathbf{I}_e(\tau))d\tau + \bar{\mathbf{M}}_s\mathbf{M}_s^{-1}\mathbf{K}_g\Omega = 0$, Then, from equations (30) and (14), we obtain

$$\begin{aligned}\bar{Y}\tilde{\Theta} &= -\hat{\mathbf{M}}_s\bar{\mathbf{M}}_s^{-1}\left\{-\bar{\mathbf{M}}_s\mathbf{M}_s^{-1}\mathbf{K}_g\Omega\right\} - \mathbf{K}_g\Omega, \\ &= \hat{\mathbf{M}}_s\mathbf{M}_s^{-1}\mathbf{K}_g\Omega - \mathbf{K}_g\Omega,\end{aligned} \tag{31}$$

By including the term $\pm\bar{\mathbf{M}}_s\mathbf{M}_s^{-1}\mathbf{K}_g\Omega$ into equation (31), it follows that

$$\bar{Y}\tilde{\Theta} = (\hat{\mathbf{M}}_s-\bar{\mathbf{M}}_s)\mathbf{M}_s^{-1}\mathbf{K}_g\Omega+\bar{\mathbf{M}}_s\mathbf{M}_s^{-1}\mathbf{K}_g\Omega-\mathbf{K}_g\Omega, \tag{32}$$

where the expression $(\hat{\mathbf{M}}_s-\bar{\mathbf{M}}_s)\mathbf{M}_s^{-1}\mathbf{K}_g\Omega$ can be included into the linearly parameterizable form as follows

$$Y\tilde{\Theta} = \bar{Y}\tilde{\Theta} - (\hat{\mathbf{M}}_s - \bar{\mathbf{M}}_s)\mathbf{M}_s^{-1}\mathbf{K}_g\Omega. \tag{33}$$

Then, from equation (32) and taking into account equation (15), it is clear that

$$\dot{\Omega} = -\mathbf{K}_g\Omega - Y\tilde{\Theta}. \tag{34}$$

Using the gradient update law

$$\dot{\tilde{\Theta}} = \Gamma^{-1}Y\Omega, \tag{35}$$

together with the following Lyapunov function

$$V_2(\Omega,\tilde{\Theta}) = \tfrac{1}{2}\Omega^T\Omega + \tfrac{1}{2}\tilde{\Theta}^T\Gamma\tilde{\Theta}, \tag{36}$$

by computing $\dot{V}_2(\Omega,\tilde{\Theta})$ along the trajectories of system (34) and substituting (35), it follows that

$$\begin{aligned}\dot{V}_2(\Omega,\tilde{\Theta}) &= \Omega^T(-\mathbf{K}_g\Omega - Y\tilde{\Theta}) + \tilde{\Theta}^T\Gamma(\Gamma^{-1}Y\Omega), \\ &= -\Omega^T\mathbf{K}_g\Omega - \Omega^TY\tilde{\Theta} + \tilde{\Theta}^TY\Omega, \\ \dot{V}_2(\Omega,\tilde{\Theta}) &= -\Omega^T\mathbf{K}_g\Omega < 0.\end{aligned} \tag{37}$$

Integrating both sides of (37) gives

$$V_2(t) - V_2(0) = -\int_0^t \Omega^T\mathbf{K}_g\Omega d\sigma < \infty. \tag{38}$$

As a consequence V_2 is a so-called square integrable function. Furthermore, Ω is square integrable and its derivative has been shown to be bounded. Then, from Lemma A1 given in appendix 1, $\Omega \to 0$ as $t \to \infty$. This shows that the controller (24) drives the tracking errors towards the impedance slave invariant manifold $I_e = 0$. **QED**

2.3 Analysis of transparency

In a bilateral teleoperation scheme the human operator and the remote environment are considered to be passive systems. Communication block between master and slave system can be analyzed as a 2-port system which transfer articular positions $(\dot{x}_m, \dot{x}_s)$ and forces $(\mathbf{f}_h, \mathbf{f}_e)$, this relation is given by a hybrid matrix given by

$$\begin{bmatrix}\mathbf{f}_h(s)\\ \dot{x}_s(s)\end{bmatrix} = \begin{bmatrix}h_{11}(s) & h_{12}(s)\\ h_{21}(s) & h_{22}(s)\end{bmatrix}\begin{bmatrix}\dot{x}_m(s)\\ -\mathbf{f}_e(s)\end{bmatrix},$$

where

$$\begin{aligned}h_{11} &= \left.\tfrac{\mathbf{f}_h(s)}{\dot{x}_m(s)}\right|_{\mathbf{f}_e=0} = \bar{M}_m s + \bar{C}_m + \tfrac{\bar{K}_m}{s},\\ h_{12} &= \left.\tfrac{\mathbf{f}_h(s)}{\mathbf{f}_e(s)}\right|_{\dot{x}_m=0} = -k_f e^{-sT},\\ h_{21} &= \left.\tfrac{\dot{x}_s(s)}{\dot{x}_m(s)}\right|_{\mathbf{f}_e=0} = k_p e^{-sT},\\ h_{22} &= \left.\tfrac{\dot{x}_s(s)}{\mathbf{f}_e(s)}\right|_{\dot{x}_m=0} = \tfrac{s}{\bar{M}_s s^2+\bar{C}_s s+\bar{K}_s}.\end{aligned}$$

This 2-port system satisfy the Llewellyn stability criterion for absolute stability if the following condition holds

$$[cos(2wT)-1]k_pk_f+\frac{2\bar{C}_m\bar{C}_sw^2}{(\bar{K}_s-\bar{M}_sw^2)^2+(\bar{C}_sw)^2}\geq 0. \tag{39}$$

If gains parameters satisfy the equation (39), then the teleoperation system is absolute stable for any $\mathbf{f}_h$ and $\mathbf{f}_e$.

3 SUPER TWISTING OBSERVER DESIGN

In this section, in order to estimate unmeasurable states of the slave system (2), the design of an observer based on sliding mode approach [18] is addressed; considering that only the position and the force applied at the slave system by the environment are available. With this aim, let us consider a nonlinear system in triangular form

$$\Sigma:\left\{\begin{array}{rcl}\dot{x}_j&=&x_{j+1},\quad j=1,...,n-1.\\ \dot{x}_n&=&\alpha(x)+\beta(x)u,\\ y&=&x_1\end{array}\right. \tag{40}$$

where $x=[x_1,\ldots,x_n]^T\in\mathcal{R}^n$ is the state vector, $y\in\mathcal{R}$ is the output vector, $u\in\mathcal{R}$ is the unknown input, and $\alpha(x)$ and $\beta(x)$ are bounded smooth scalar functions. Now assume that the state of the system is uniformly bounded, i.e. $\forall t>0, |x_i(t)|<d_i$, and $\forall t>0$. Thus, the state and its derivatives are bounded.

Then, the following system $\mathcal{O}$ is an observer for system (40)

$$\mathcal{O}:\left\{\begin{array}{rcl}\dot{\hat{x}}_1&=&\tilde{x}_2+\lambda_1|e_1|^{\frac{1}{2}}sign(e_1),\\ \dot{\hat{x}}_2&=&\alpha_1 sign(e_1),\\ \dot{\hat{x}}_2&=&E_1\left[\tilde{x}_3+\lambda_2|e_2|^{\frac{1}{2}}sign(e_2)\right],\\ &\vdots&\\ \dot{\hat{x}}_{n-1}&=&E_{n-3}\alpha_{n-2}sign(e_{n-2}),\\ \dot{\hat{x}}_{n-1}&=&E_{n-2}\left[\tilde{x}_n+\lambda_{n-1}|e_{n-1}|^{\frac{1}{2}}sign(e_{n-1})\right],\\ \dot{\hat{x}}_n&=&E_{n-2}\alpha_{n-1}sign(e_{n-1}),\\ \dot{\hat{x}}_n&=&E_{n-1}\left[\tilde{\theta}+\lambda_n|e_n|^{\frac{1}{2}}sign(e_n)\right],\\ \dot{\tilde{\theta}}&=&E_{n-1}\alpha_n sign(e_n),\end{array}\right. \tag{41}$$

where $e_i=\tilde{x}_i-\hat{x}_i$ for $i=1,\ldots,n$; with $\tilde{x}_1=x_1$ and $\left[\tilde{x},\tilde{\theta}\right]^T=\left[\tilde{x}_1,\tilde{x}_2,\ldots,\tilde{x}_n,\tilde{\theta}\right]^T$ is the output of the observer. For $i=1,\ldots,n-1$; the scalar functions E_i are defined as

$$E_i=1 \text{ if } |e_j|=|\tilde{x}_j-\hat{x}_j|\leq\varepsilon_i,\forall j\leq i;\ \text{else } E_i=0, \tag{42}$$

where ε_i is a small positive constant, while $\lambda_i>0$ and $\alpha_i>0$ are the observer gains. The convergence of the estimation error is obtained in $(n-1)$ steps in finite time [18], through a recursive scheme (41) used to reconstruct the non-measurable variables as exact differentiation with finite-time convergence [19]. With this purpose, a change of coordinates for the slave system (2) is defined as $\mathbf{X}_{s1}=\mathbf{q}_s$; $\mathbf{X}_{s2}=\dot{\mathbf{q}}_s$. Then, (2) can be rewritten in the following state space representation

$$\Sigma_s:\left\{\begin{array}{rcl}\dot{\mathbf{X}}_{s1}&=&\mathbf{X}_{s2},\\ \dot{\mathbf{X}}_{s2}&=&\mathbf{M}_s^{-1}(\mathbf{X}_{s1})\{-\mathbf{C}_s(\mathbf{X}_{s1},\mathbf{X}_{s2})\mathbf{X}_{s2}\\ &&-\mathbf{g}_s(\mathbf{X}_{s1})+\mathbf{u}_s-\mathbf{f}_h\},\end{array}\right. \tag{43}$$

which can be rewritten in the canonical form similar to (40) as follows,

$$\Sigma_s:\left\{\begin{array}{rcl}\dot{\mathbf{X}}_{s1}&=&\mathbf{X}_{s2},\\ \dot{\mathbf{X}}_{s2}&=&\mathbf{F}(\mathbf{X}_{s1},\mathbf{X}_{s2},\mathbf{f}_h)+\Delta,\end{array}\right. \tag{44}$$

where $\Delta=\mathbf{M}_s^{-1}\{\mathbf{u}_s\}$ and $\mathbf{F}(\mathbf{X}_{s1},\mathbf{X}_{s2},\mathbf{f}_h)=-\mathbf{M}_s^{-1}\{\mathbf{C}_s(\mathbf{X}_{s1},\mathbf{X}_{s2})\mathbf{X}_{s2}-\mathbf{g}_s(\mathbf{X}_{s1})+\mathbf{f}_h\}$.

Suppose that the system states are bounded, then there exists a constant f such that the inequality $\|\mathbf{F}(\mathbf{x}_1,\mathbf{x}_2,\mathbf{f}_h)\|<f$ holds for any state. Furthermore, Δ is considered as an uncertain term depending on the time delayed signals which are assumed uniformly bounded in a compact set, i.e. $\|\Delta\|\leq\alpha$, and thus the slave system is observable.

Then, the proposed super twisting observer has the following form

$$\widetilde{\mathcal{O}}:\left\{\begin{array}{l}\dot{\hat{\mathbf{X}}}_{s1}=\tilde{\mathbf{X}}_{s2}+\Lambda_1|\tilde{\mathbf{X}}_{s1}-\hat{\mathbf{X}}_{s1}|^{\frac{1}{2}}sign(\tilde{\mathbf{X}}_{s1}-\hat{\mathbf{X}}_{s1}),\\ \dot{\hat{\mathbf{X}}}_{s2}=\alpha_1 sign(\tilde{\mathbf{X}}_{s1}-\hat{\mathbf{X}}_{s1}),\\ \dot{\hat{\mathbf{X}}}_{s2}=\mathbf{E}_1[\tilde{\Theta}_1+\Lambda_2|\tilde{\mathbf{X}}_{s2}-\hat{\mathbf{X}}_{s2}|^{\frac{1}{2}}sign(\tilde{\mathbf{X}}_{s2}-\hat{\mathbf{X}}_{s2})],\\ \dot{\tilde{\Theta}}_1=\mathbf{E}_2\alpha_2 sign(\tilde{\mathbf{X}}_{s2}-\hat{\mathbf{X}}_{s2}),\\ \dot{\hat{\mathbf{X}}}_{s3}=\mathbf{E}_2[\tilde{\Theta}_2+\Lambda_3|\tilde{\mathbf{X}}_{s3}-\hat{\mathbf{X}}_{s3}|^{\frac{1}{2}}sign(\tilde{\mathbf{X}}_{s3}-\hat{\mathbf{X}}_{s3})],\\ \dot{\tilde{\Theta}}_2=\mathbf{E}_3\alpha_3 sign(\tilde{\mathbf{X}}_{s3}-\hat{\mathbf{X}}_{s3}),\end{array}\right. \tag{45}$$

where $\hat{\mathbf{X}}_{s1}$ and $\hat{\mathbf{X}}_{s2}$ are the state estimations of the state vectors $\mathbf{X}_{s1}$ and $\mathbf{X}_{s2}$, $\Lambda_1=diag\{\lambda_{1,1},...,\lambda_{n,1}\}$, $\Lambda_2=diag\{\lambda_{1,2},...,\lambda_{n,2}\}$, $\alpha_1=diag\{\alpha_{1,1},...,\alpha_{n,1}\}$ and $\alpha_2=diag\{\alpha_{1,2},...,\alpha_{n,2}\}$ are the gains of the observer; $\tilde{\mathbf{X}}_{s1}=\mathbf{X}_{s1}, |\tilde{\mathbf{X}}_{s1}-\hat{\mathbf{X}}_{s1}|^{\frac{1}{2}}=diag\left\{|\tilde{\mathbf{x}}_{s1,1}-\hat{\mathbf{x}}_{s1,1}|^{\frac{1}{2}},...,|\tilde{\mathbf{x}}_{s1,n}-\hat{\mathbf{x}}_{s1,n}|^{\frac{1}{2}}\right\}, sign(\tilde{\mathbf{X}}_{s1}-\hat{\mathbf{X}}_{s1})=diag\left\{sign(\tilde{\mathbf{x}}_{s1,1}-\hat{\mathbf{x}}_{s1,1}),...,sign(\tilde{\mathbf{x}}_{s1,n}-\hat{\mathbf{x}}_{s1,n})\right\}$.

Observer $\widetilde{\mathcal{O}}$ estimates velocity $\dot{\mathbf{x}}_s$ and acceleration $\ddot{\mathbf{x}}_s$ of the slave system, using only information of position $\mathbf{x}_s$ and environment force $\mathbf{f}_e$. Notice that, the time delayed signals appear in the system in such a way that it can be concentrated in a term which can be bounded by a constant.

Proposition 4.1. Consider slave system (43), and suppose that only position $\mathbf{X}_{s1}$ and environment force $\mathbf{f}_e$ are available. Under the assumption that the time delayed signals are bounded and the time delay is constant but unknown, the system (45) is an observer for system (43). Moreover, the states of the observer converge in finite-time to the states of the system (43).

Proof. The convergence in finite-time of the observer can be straightforward proved following the same procedure given in [18]. **QED**

The following theorem ensures the stability of the closed-loop system using the proposed control scheme.

Theorem 1 *Consider the slave system (43) in closed-loop with the impedance control (8), using the estimated states given by the super twisting observer (45), under time delayed signals of master-slave. Then, the closed-loop slave system is exponentially stable. Furthermore, slave system tracks the time delayed trajectories of master system.*

Proof. Due to the finite-time convergence property of the observer, the separation principle is accomplished. Then, observer and control systems can be designed separately. Since the slave control has been designed to stabilize the slave system, the stability of the closed-loop system is proved. **QED**

4 EXPERIMENTAL RESULTS

In this section, experimental results obtained by the implementation of the proposed control scheme in a teleoperation platform are presented. Due to hardware limitations, two experimental cases were considered: For the first case, a platform composed of two physical robots of 1-DOF is considered (see Figure 2). For the second case, a virtual master and a physical 2-DOF slave robot are considered (see Figure 7). Manipulators are connected to a PC through a *NI 6033E* acquisition card. *LabView* software is used to handle signals and to process controller and observer algorithms in a real time environment, with real time threads to enforce constant bandwidth and monitor all latencies to guarantee a hard real time environment. The sample time was fixed to $T_s = 0.001$ seconds. A couple of servopacks *SGDH-02BE Yaskawa* 100V AC, together with two servomotors embedded encoders *SGMAH-02F41* and a *JR3-67M25A* force and torque sensor. Position information is provided by encoders fitted on each motor.

4.1 First case - 1-DOF robots

The parameters used for the 1-DOF experiment are presented in Table 1. Impedance desired parameters were chosen heuristically similar to those measured for the robot.

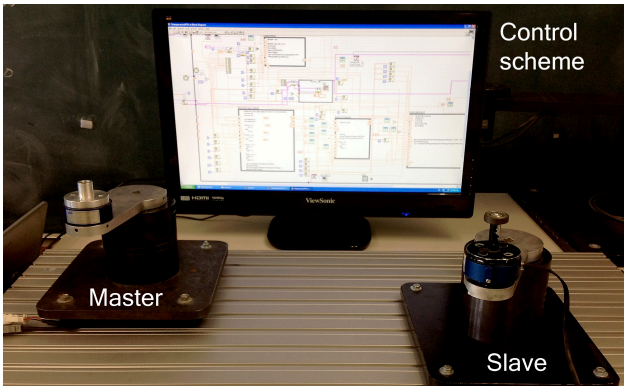

Fig. 2: Teleoperation platform for first experimental case.

Control parameters are selected as $k_p = 1$, $k_i = 1$, $k_g = 0.001$. The observer gains are chosen as $\lambda_1 = 30$, $\lambda_2 = 75$, $\lambda_3 = 130$, $\alpha_1 = 250$, $\alpha_2 = 150$ and $\alpha_3 = 200$. Moreover, E_1 is selected according to condition (42), $\varepsilon_1 = 0.01$ and $\varepsilon_2 = 0.05$.

The proposed scheme is implemented with the aim of tracking a desired reference generated by $\mathbf{f}_h$, which is applied manually to the master robot.

The dynamics of the complete scheme are plotted in Figure 3. As can be seen, position, velocity and acceleration of the slave system track the reference generated by the master, without time delay. Slave control uses estimates of velocity and acceleration having a stable behavior. Sensors are used for comparison, as can be seen observer estimates overcome noisy measurements which are very critical in practical implementations. Furthermore, the complete scheme is stable when its applied an external $\mathbf{f}_e$ force.

On the other hand, in Figure 4 can be seen the performance of the complete scheme under time delay $T_1 = T_2 = T_d = 2$. Further experiments have shown that time delay is especially important when an environmental force $\mathbf{f}_e$ appears, i.e. a huge time delay may decrease the performance of this scheme. In both cases, experiments have

Master parameters	
$m_m = 0.0006kg$	$\bar{c}_m = 0.2N \cdot s/m$
$\bar{m}_m = 0.0005kg \cdot m^2$	$\bar{k}_m = 0.9N/m$
$c_m = 0.0658N \cdot s/m$	$k_f = 0.1N \cdot m$
Slave parameters	
$m_s = 0.0006kg$	$\bar{c}_s = 0.15N \cdot s/m$
$\bar{m}_s = 0.0005kg \cdot m^2$	$\bar{k}_s = 1.5N/m$
$c_s = 0.0658N \cdot s/m$	

Table 1: System parameters for first case.

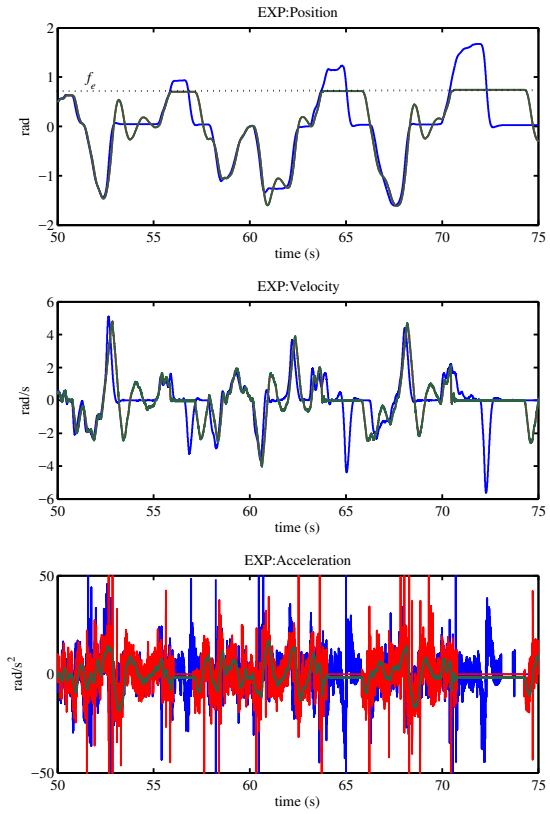

Fig. 3: 1st case: Dynamics of master (blue), slave (red) and estimated (green) without time delay and in presence of an external force $\mathbf{f}_e$.

been done considering an arbitrary reference $\mathbf{f}_h$ given by the human operator. A force cell was implemented to measure this signal. In Figure 5, master and slave controls are plotted using a time delay $T_d = 2s$.

Finally, in Figure 6, the estimated errors for velocity and acceleration are shown.

4.2 Second case - 2-DOF robots

The parameters used for the 2-DOF experiment are presented in Table 2.

Impedance desired parameters were chosen according to Llewellyn criterion (39). Observer gains were chosen as follows $\alpha_1 = 385\mathbf{I}, \alpha_2 = 650\mathbf{I}, \alpha_3 = 900\mathbf{I}, \Lambda_1 = 25\mathbf{I}, \Lambda_2 = 40\mathbf{I}, \Lambda_3 = 90\mathbf{I}$. Moreover E_1, E_2 and E_3 were selected according to condition (42) and choosing $\varepsilon_1 = 0.01$, $\varepsilon_2 = 0.05$ and $\varepsilon_2 = 0.01$.

The proposed scheme is implemented for tracking a desired reference generated by f_h, which is applied at the

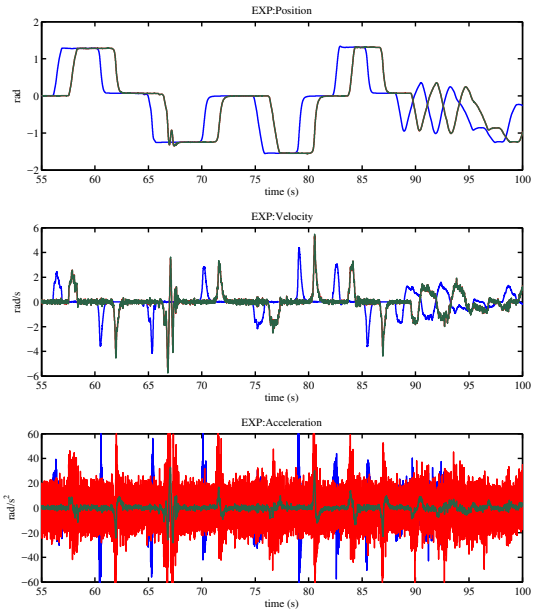

Fig. 4: 1st case: Dynamics of master (blue), slave (red) and estimated (green) with a time delay of $T_d = 2s$.

master robot. In the Figure 8 is shown the position of the master and slave robots and furthermore the environment force f_e, where the high-end sensor measures between slave system and the environment. Moreover, the remote force f_e affects the trajectory of the master from $149s$ to $154s$, which is sent to the operator.

From experiments can be seen that when a high contact force f_e is applied, a bouncing appears on master side if the operator is not applying any force when f_e is received. This becomes critical under large time delays.

In Figure 9 can be appreciated how velocity of the slave system tracks the reference generated by the master, for a constant time delay of $T_d = 2s$. Notice that the proposed controller only uses information provided by the sliding

Master parameters	
$\bar{\mathbf{M}}_m$ =	diag (0.7 , 0.87) kg
$\bar{\mathbf{C}}_m$ =	diag (1.2 , 1.0) N· s / m
$\bar{\mathbf{K}}_m$ =	diag (1.1 , 1.02) N / m
Slave parameters	
$\mathbf{M}_s$ =diag(0.02 , 0.06)kg	$\mathbf{K}_p = \mathbf{I}$
$\bar{\mathbf{C}}_s$ =diag(0.9 , 0.9)N· s / m	$\bar{\mathbf{K}}_i$ =diag(10.0 , 35.0)
$\bar{\mathbf{K}}_s$ =diag(2.5 , 2.5)N / m	$\bar{\mathbf{K}}_g$ =diag(0.01 , 0.001)

Table 2: System parameters for second case.

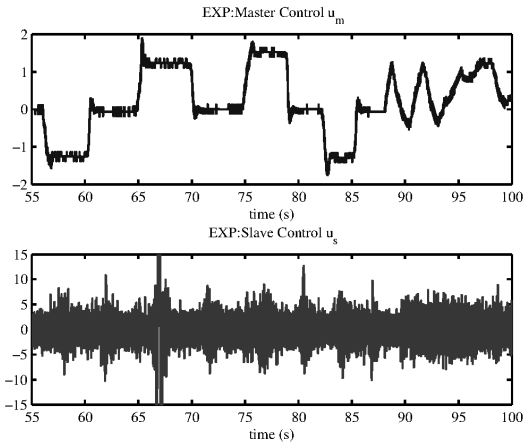

Fig. 5: 1st case: Control signal for master (top) and slave (bottom) system with a time delay $T_d = 2s$.

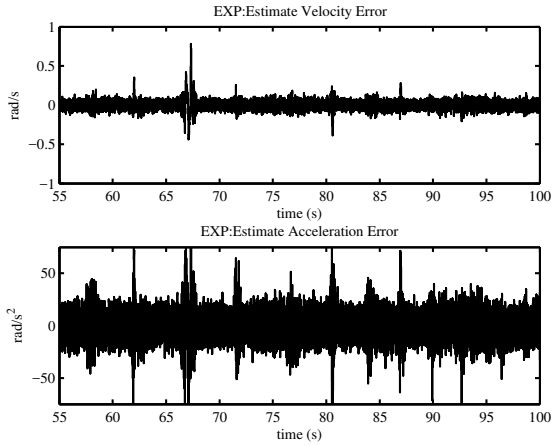

Fig. 6: 1st case: Velocity (top) and acceleration (bottom) estimation errors, with a time delay $T_d = 2s$.

mode observer, while velocity and acceleration sensors are just used for comparison. Figure 10 shows the acceleration of master, slave and its estimation; while on bottom, a zoomed view of the observer estimation of acceleration can be appreciated. In the Figure 11, master and slave control signals are plotted. Oscillations on slave control signal mainly come from measurement noise and delayed signals from master. In the second experimental case, since a virtual master has been used the master signals do not contain measurement noise. Then, the slave control signal is significantly smoother than first experimental case where an important component of noise in master signal is present.

Furthermore, the performance of the super twisting observer is shown in Figure 12, where position and velocity errors are plotted. As can be seen, estimates of the position and velocity show less peaking phenomena.

Now, for the second experimental case, the following inputs have been considered:

- *Input 1*: A human operator applies a sinusoidal force f_h to the system with a time-delay of $T_d = 250ms$ (see Figure 13).
- *Input 2*: An arbitrary reference given by the human operator is given with a time delay of $T_d = 500ms$ (see Figure 14).

5 CONCLUSIONS

In this work, a nonlinear control scheme for bilateral teleoperated system based on sliding mode techniques in presence of unknown and constant time delays in the communication channel has been presented. An impedance

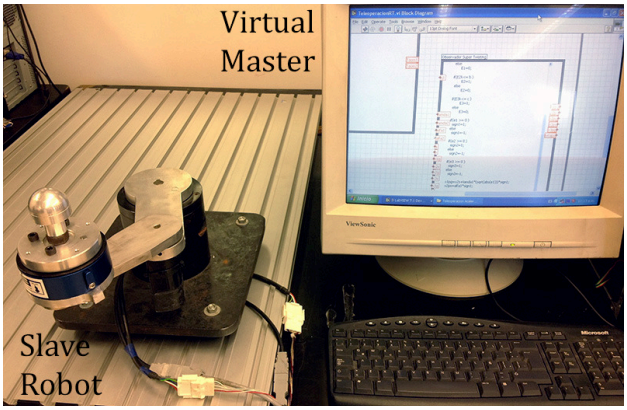

Fig. 7: Teleoperation platform for second experimental case.

controller combined with a second order sliding mode observer has been applied to a slave system in order to track the position, velocity and contact force delayed signals sent by a master system. An analysis of the stability of the system has been given, where sufficient conditions have been obtained to guarantee the stability of the closed loop. Experimental results have been obtained to illustrate the performance of the proposed approach under parametric uncertainties and measurement noise.

ACKNOWLEDGMENT

This work was partially supported by the Mexican CONACYT (Ciencia Básica) under Grant No. 105799, and the Project PAICYT-UANL.

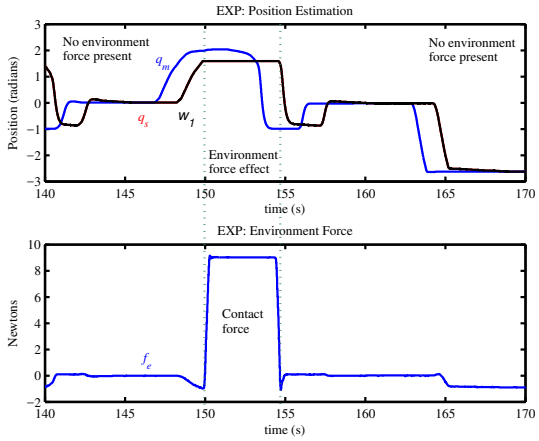

Fig. 8: 2nd case: Position of master and slave systems under a time delay of $T_d = 2s$ and an external f_e force. Master (blue), slave (red) and estimated (black).

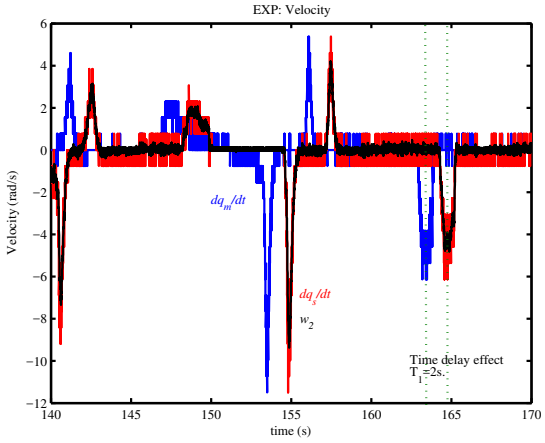

Fig. 9: 2nd case: Velocity of master and slave systems under a time delay of $T_d = 2s$ and an external f_e force. Master (blue), slave (red) and estimated (black).

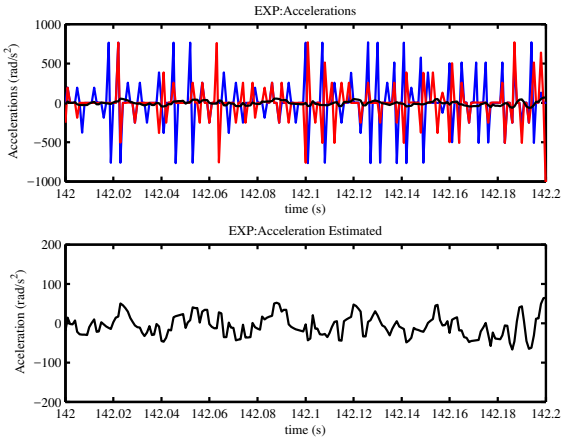

Fig. 10: 2nd case: Acceleration of master (blue), slave (red) and estimated (black) under a time delay of $T_d = 2s$.

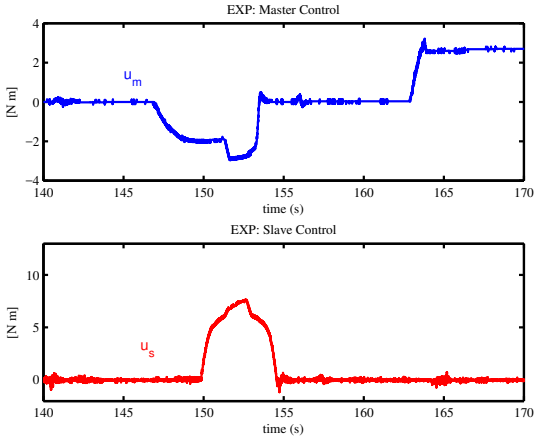

Fig. 11: 2nd case: Control signal for master and slave system for second experiment.

REFERENCES

[1] P. Hokayem and M. Spong: Bilateral teleoperation: an historical survey. Automatica *42* (2006), 12, pp. 2035-2057.

[2] J. Guo, S. Guo, N. Xiao, B. Gao, M. Xu and M. Qu: A method of decreasing time delay for a tele-surgery system. International Conference on Mechatronics and Automation (ICMA) 2012, pp. 1191-1195.

[3] J. Daly, M. Ya and S. Waslander: Coordinated landing of a quadrotor on a skid-steered ground vehicle in the presence of time delays, IEEE/RSJ International Conference on Intelligent Robots and Systems (IROS), 2011, pp. 4961-4966.

[4] N. Chopra, M. Spong and R. Lozano: Synchronization of bilateral teleoperators with time delay. Automatica *44* (2008), 8, pp. 2142-2148.

[5] E. Nuño, L. Basañez, R. Ortega and M. Spong: Position tracking for nonlinear teleoperators with variable time-delay. The International Journal of Robotics Research *28* (2009), 7, pp. 895-910.

[6] E. Nuño, R. Ortega and L. Basañez: An adaptive controller for nonlinear teleoperators. Automatica *46* (2010), 1, pp. 155-159.

[7] A. Lopes and F. Almeida: Acceleration Based Force-Impedance Control of a 6-dof Parallel Robotic Manipulator, IEEE Int. Conf. on Computational Cybernetics 2006, pp. 1-6.

[8] F. Mobasser, K. Hashtrudi-Zaad and S. Salcudean: Impedance Reflecting Rate Mode Teleoperation, Proc. IEEE International Conference on Robotics and Automation, Taiwan 2003, pp. 3296-3302.

[9] A. Hace, M. Franc and K. Jezernik: Sliding mode control for scaled bilateral teleoperation, IECON 2011 - 37th Annual

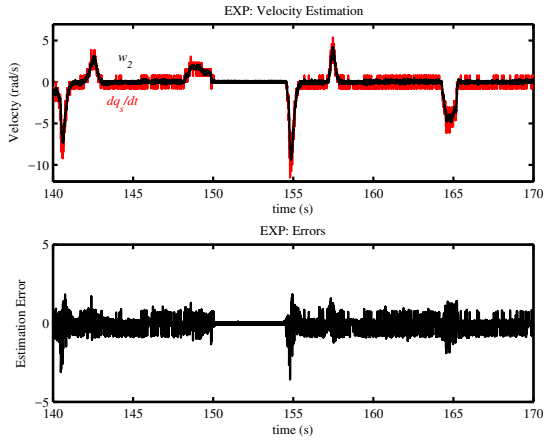

Fig. 12: 2nd case: Velocity and its estimation error. Slave velocity (red) and observer estimation (black).

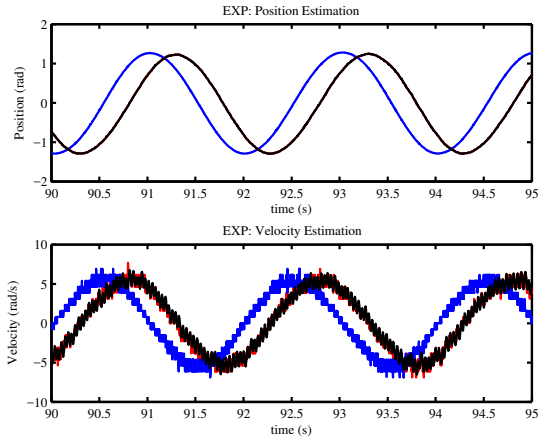

Fig. 13: 2nd case: Position and velocity estimation error, for a sinusoidal signal with a time-delay of $T_d = 250ms$. Master (blue), slave (red) and estimated (black).

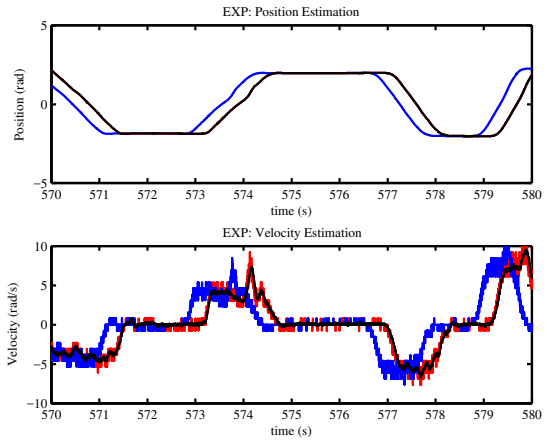

Fig. 14: 2nd case: Position and velocity estimation error, for a random signal with a time-delay of $T_d = 500ms$. Master (blue), slave (red) and estimated (black).

Conference on IEEE Industrial Electronics Society 2011, pp. 3430-3435.

[10] Y. Xia, M. Fu, H. Yang and G. Liu: Robust Sliding-Mode Control for Uncertain Time-Delay Systems Based on Delta Operator. IEEE Transactions on Industrial Electronics, *56* (2009), 9, pp. 3646-3655.

[11] L. García-Valdovinos, V. Parra-Vega and M. Arteaga: Observer-based sliding mode impedance control of bilateral teleoperation under constant unknown time delay. Robotics And Autonomous Systems *55* (2007), pp. 609-617.

[12] J. Ryu and D. Kwon: A novel adaptive bilateral control scheme using similar closed-loop dynamic characteristics of master/slave manipulators. J. Robot. Syst. *18* (2001), 9, pp. 533-543.

[13] W. Zhu and S. Salcudean: Stability guaranteed teleoperation: An adaptive motion/force control approach. IEEE Trans. Automatic Control *45* (2000), pp. 1951-1969.

[14] S. Drakunov, W. Perruquetti, J.Richard and L. Belkoura: Delay Identification In Time-Delay Systems using Variable Structure Observers. Annual Reviews In Control *30* (2006), 2, pp. 143-158.

[15] M. Lum, J. Rosen, T. Lendvay, A. Wright, M. Sinanan and B. Hannaford: Telerobotic Fundamentals of Laparoscopic Surgery (FLS): Effects of time delay - pilot study, Engineering in Medicine and Biology Society 30th Annual International Conference of the IEEE 2008, pp. 5597-5600.

[16] S. Ibrir: Observer-based control of a class of time-delay nonlinear systems having triangular structure. Automatica *47* (2011), 2, pp. 388-394.

[17] M. Ibrir: Adaptive observers for time-delay nonlinear systems in triangular form. Automatica *45* (2009), 10, pp. 2392-2399.

[18] T. Floquet and J. Barbot: Super twisting algorithm based step-by-step sliding mode observers for nonlinear systems with unknown inputs. International Journal of Systems Science *38* (2007), pp. 803-815.

[19] T. Floquet, C. Edwards and S. Spurgeon: On Sliding Mode Observers for Systems with Unknown Inputs. Variable Structure Systems (2006), pp. 214-219.

[20] J. Davila, L. Fridman and A. Levant: Second-order sliding-mode observer for mechanical systems. IEEE Transactions on Automatic Control (2005), pp. 1785-1789.

[21] M. Ezzat, J. DeLeón, N. González and A. Glumineau: Sensorless speed control of permanent magnet synchronous motor by using sliding mode observer, 11th International Workshop on Variable Structure Systems (VSS), 2010, pp. 227-232.

Nicolás González N. González received the B.S. degree in electronics and communications and the M.Sc. Degree in Electrical Engineering with specialty in Automatic Control, from the Universidad Autónoma de Nuevo León, in 2002 and 2005 respectively. He is currently working towards the Ph.D. degree at the Universidad Autónoma de Nuevo León. His main interests are robotics, control theory and its applications.

Oscar Salas-Peña O. Salas received the B.Sc. degree in computer science, M.Sc. and Ph.D. degrees in electrical engineering from Universidad Autónoma de Nuevo León, in 2004, 2006 and 2013 respectively. Since 2014, he has been a Professor of Mechatronic Engineering with the Universidad Autónoma de Nuevo León, Mexico. He is currently working on applications of control theory, nonlinear observers, electromechanical systems and unmanned aerial vehicles.

Jesús de León-Morales J. de León received the Ph.D. degree in automatic control from Claude Bernard Lyon 1 University, Villeurbanne, France, in 1992. Since 1993, he has been a Professor of Electrical Engineering with the Universidad Autónoma de Nuevo León, San Nicolás de Los Garza, Mexico. He is currently working on applications of control theory, electrical machines, nonlinear observers and power systems.

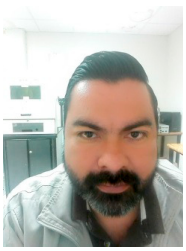

Sergio Rosales S. Rosales received the B.Sc. degree on electronics from the Technical Institute of Saltillo, Mexico, in 2006. The M.Sc. degree on Robotics and advanced manufacture from Research Center for Advanced Studies (CINVESTAV), Saltillo, Mexico, in 2009. He is currently working towards the Ph.D. degree at CINVESTAV. His main research interests include robotics, teleoperation and robots formations.

Vicente Parra-Vega V. Parra-Vega received two B.S. degrees one in control and computing, and the other in electronics and communications, from the Universidad Autónoma de Nuevo León, Mexico, in 1987. The M.Sc. degree in automatic control from the Research Center for Advanced Studies (CINVESTAV), Mexico, in 1989, and the Ph.D. degree in mathematical engineering and information physics from the University of Tokyo, Japan, in 1995. Since 1999 he has been with the Mechatronics Division of CINVESTAV, where he is currently a professor and director of the robotics and manufacturing laboratory.

AUTHORS' ADDRESSES

Nicolás González, M.Sc.[1]
Oscar Salas-Peña, Ph.D.[2]
Jesús de León-Morales, Ph.D.[1]
Sergio Rosales, M.Sc.[3]
Vicente Parra-Vega, Ph.D.[3]
[1]**Department of Electrical Engineering,**
[2]**Department of Mechatronics Engineering,**
Faculty of Mechanical and Electrical Engineering,
Universidad Autónoma de Nuevo León,
San Nicolás de Los Garza, 66451, Mexico
email: nicolasgzz@gmail.com, salvador.sp@gmail.com, drjleon@gmail.com
[3]**Robotics and Advanced Manufacturing Division,**
Research Center for Advanced Studies,
Saltillo, 25900, Mexico
email: wildsarm@gmail.com, vparra@cinvestav.mx

Received: 2015-07-10
Accepted: 2016-08-29